*Netherlands Journal of Agricultural Science 42-4 (1994) 271-292*

# Composting of mushroom substrate in a fermentation tunnel: compost parameters and a mathematical model

J.J.C. VAN LIER[1], J.T. VAN GINKEL[2], G. STRAATSMA[1†], J.P.G. GERRITS[1] AND L.J.L.D. VAN GRIENSVEN[1]

[1] Mushroom Experimental Station, P.O. Box 6042, NL–5960 AA Horst, The Netherlands
[2] DLO Research Institute for Agrobiology and Soil Fertility (AB-DLO), P.O. Box 129, NL-9750 AC Haren, The Netherlands

Received 27 January 1993; accepted 17 July 1994

## Abstract

Phase II of composting of mushroom substrate was studied in bulk fermentation tunnels. Compost data are given on heat production, settling and mass reduction, porosity and thermal conductivity. Mass and moisture determinations at the end of the process revealed slightly positive gradients in the direction of the air stream. The highest rate of degradation occurred during the first 2 days. A mathematical model of mass and heat transfers was made for a better understanding of the complex composting process. Differential equations were solved with time-dependent analysis using a Continuous Simulation and Modelling Program (CSMP). In the calculations, the substrate was divided into theoretical layers of equal thickness but of different density and porosity. The model predicts the time-course of the process taking into account the moisture content and the filling height of the compost, and the amounts of supplied fresh air and recirculated air. The calculated data include the oxygen demand, the water and dry matter losses, the temperatures in the various layers, and the loss of conductive heat through the walls of the containers in the tunnel. Calculated data corresponded with actual process data. Temperatures were correct within 3 °C and weight losses within 5%.

*Keywords*: biotechnology, aerobic indoor composting, model description, mushroom compost, forced convection, solid state fermentation

## Introduction

The preparation of compost for the production of the white button mushroom *Agaricus bisporus* is a commercially important solid-state fermentation process, which is based on microbial degradation and self-heating. Compost consists of a mixture of wheat straw, horse manure, broiler chicken manure, gypsum and water

† corresponding author

(Gerrits, 1988a). Phase I and Phase II composting can be distinguished (Sinden & Hauser, 1950). Heaps of raw materials are prewetted and mixed for 1–2 weeks. Then Phase I of outdoor composting is implemented in long rows for about 1 week. Unpleasant-smelling compounds (Derikx *et al.*, 1990a) and 2.1 kg tonne$^{-1}$ of $NH_3$ are emitted (Gerrits & Van Griensven, 1990). Phase II is an indoor process of pasteurization at 56 °C, followed by conditioning at 45 °C for 7 days. During Phase II an additional 0.2 kg tonne$^{-1}$ of $NH_3$ is emitted (Gerrits, 1988a) and thermophilic fungi develop that are indispensable for later mushroom production (Straatsma *et al.*, 1989). Phase II can either be performed in mushroom houses in beds or trays, or in bulk in special solid-state fermentation rooms, commonly designated as tunnels. In both cases the self-heating of the substrate is controlled by ventilating air. In tunnels, the air is forced through the compost (convection), allowing an accurate control (Gerrits, 1988a). Both temperature and $O_2$ concentration may be used to regulate the convection rate through the compost. Experiments with continuous forced convection showed a maximum $O_2$ consumption at 55 °C (Spohn, 1970), which is consistent with *in vitro* data (Derikx *et al.*, 1990b).

Mass and heat transfers influence the progress of composting. We assume that the energy produced results from cellulose degradation. Hemicellulose degradation is also important (Gerrits *et al.*, 1967), its degradation being similar. Overall calculations on mass and heat transfers were given by Randle (1977). Hogan *et al.* (1989) compared the thermodynamics of a laboratory-scale composting chamber with a field scale system using a mathematical model.

Experimental data from our tunnels during Phase II composting revealed the following parameter ranges in order to produce maximum mushroom yields (Gerrits, 1988a): pasteurization temperature between 55 and 63 °C, conditioning temperature between 40 and 48 °C, air flow between 120 to 200 m$^3$ h$^{-1}$ tonne$^{-1}$, oxygen concentration between 15 and 20% (v/v) and initial moisture content approximately 75% (w/w).

The importance of composting in tunnels will increase since both Phase I and Phase II have to be carried out in tunnels in the near future, to avoid emission of stench and ammonia. We consider modelling to be helpful in understanding the complex composting process in tunnels and in revealing the interrelations of the process parameters.

## Materials and methods

### *The tunnel process*

The 4 tunnels at the Mushroom Experimental Station (Figure 1) each hold 4 stainless steel containers. A container has a grid floor for the entrance of air (25% open) and two adjustable front panels; its dimensions are 1.03 × 1.03 × 1.82 m (L × W × H); it holds 1000 kg of substrate initially. The tunnels are insulated with polyurethane panels.

Self-heating of the substrate is used to reach and to maintain the desired process

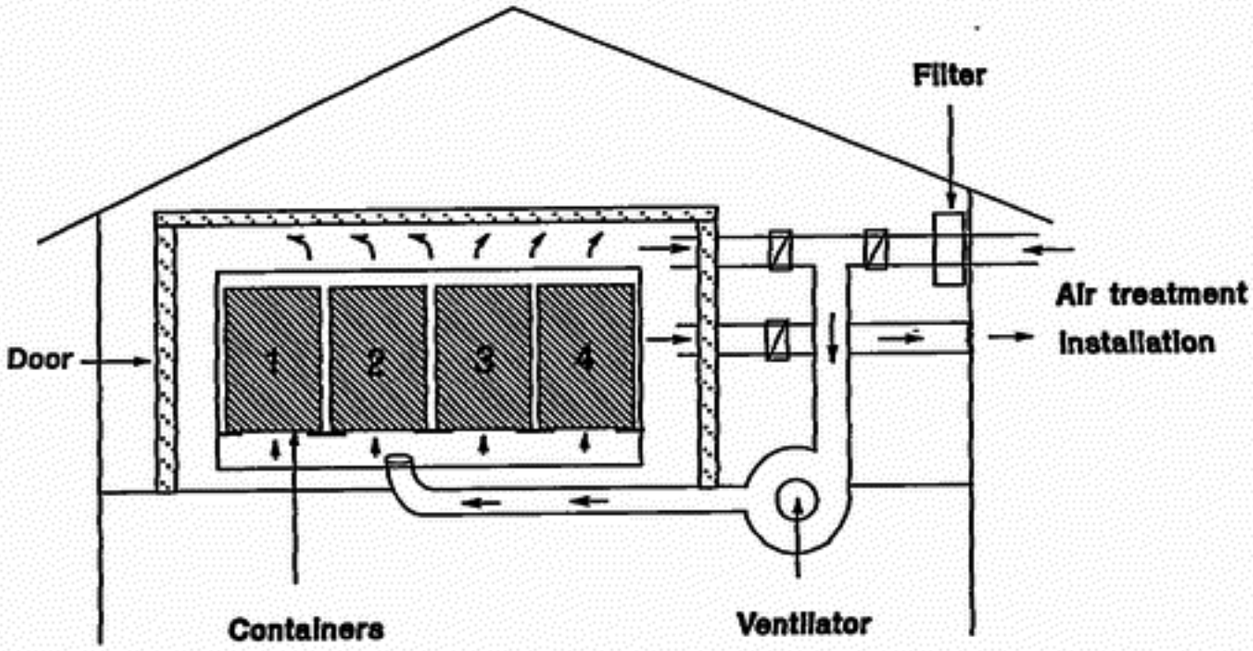


Figure 1. Diagram of four containers in a tunnel at the Mushroom Experimental Station.

temperatures. If necessary, steam can be added. A fan supplies maximally 200 $m^3$ $tonne^{-1}$ $h^{-1}$ of air, variable in temperature and in moisture content, through the bulk of the substrate in upward direction. After passage through the compost, air is returned. At the start of Phase II the substrate temperature is regulated to increase at 2.5 °C $h^{-1}$. After about 10 h the pasteurization temperature of 56 °C in the compost is reached and maintained at that level for 8 h. Then the substrate is cooled at 3 °C $h^{-1}$ until the conditioning temperature of 45 °C is reached and maintained at that level for about 6 days. The composting process is controlled by ventilative heat management; i.e. temperature data of compost, return air and fresh air are processed by a computer to regulate the admittance of fresh air according to the programmed progress of composting. In the return and supply ducts the quantities of air are measured with a flange. Fresh air is filtered for hygienic reasons. Anaerobiosis is prevented by the high air circulation rate; the $CO_2$ concentration rises to values between 6% and 10% (Gerrits, 1988b). $O_2$ or $CO_2$ controls for process management may be useful only at the start of Phase II when temperature is allowed to increase for pasteurization.

After about 7 d, the ammonia concentration in the supply air has dropped below 10 ppm, and Phase II is finished. The tunnels are emptied, and the compost is ready for the cultivation of *Agaricus bisporus*.

*Compost recipe*

Unless stated otherwise, straw compost and horse manure compost (Gerrits, 1988a) were used. Ingredients for ample 1000 kg straw compost are: 250 kg chopped wheat straw (length 5–10 cm; 15% moisture, w/w), 125 kg broiler chicken manure (38% moisture, w/w), 20 kg gypsum (10% moisture, w/w) and 1100 L water. Recipe for ample 1000 kg horse manure compost: 800 kg horse manure (60% moisture w/w), 80

kg broiler chicken manure, 20 kg gypsum and 240 L water. The mixed ingredients are stacked in a row (2 × 0.7 × 0.6 m, L × W × H) for 5 days prior to usage in the tunnel.

*Routine analysis of compost and process parameters*

Standard sampling of compost was done at the beginning and at the end of trials. From a mixed sample, 3 aliquots of max 250 g were analyzed for dry matter and moisture content. These samples were dried in an oven for 12 h at 105 °C and the weight loss was determined (Mettler, 0.05 g accuracy).

Temperatures in the supply and return air in the top of one container, and in the ambient air outside the tunnel plant were monitored every 5 min using PT100 elements. The data were stored in a PC (Hewlett Packard 9816), which was also used to control the process. Temperatures in the compost at 20 cm from the bottom and at 10 cm from the top of each container, and the temperature of the supply and return air were also monitored by a second set of PT100 elements connected to data-takers (Data Logger, DT 1001) and stored in a portable PC (Supercom LCD-286). The amount of supply air and the pressure difference between the supply and return air were monitored every 5 min. $CO_2$ and $O_2$ concentrations were measured under and above the containers with a Siemens Ultramat 22P (0–4% $CO_2$ or 0–20% $CO_2$) and a Siemens Oxymat 2 (0–21% $O_2$) (accuracy of both 0.1%).

*Determination of compost parameters used in the model*

*Density, porosity, and moisture in relation to height.* A container was filled with 10 layers of 100 kg of compost, separated by nylon nets (1 × 1 cm mesh). After settling, the height of the layers was measured. From this the density $\rho_c$ of the layers was calculated. The layers were weighed and sampled at the end of the process for moisture and dry matter analysis to determine gradients in the compost.

*Settling of compost, weight reduction and heat production.* In trial 1447, straw composts with moisture contents of 71.2, 74.6, 77.9 and 80.5% (w/w) were used. Extra temperature monitoring was done on three different spots in every front container in the tunnel at 30 cm from the surface in the compost. Moisture samples in triplo were taken at 30 cm from the surface of the compost every 24 h. At the same moment, weight and height of the compost was measured. The dry matter conversion rate was calculated from the weight and moisture data. Based on the assumption that only cellulose was converted (Equation 7) the heat production $W$ at the measured temperature was calculated and plotted as a function of process time.

*Thermal conductivity.* Thermal conductivity of compost was measured with a lambda needle (TFDL Wageningen, DCL-10). Procedure and calculations were done according to Van Loon (1991). We used a Dewar vessel (2.36 L; 5 × 30 cm, r × H) filled by hand with 1272 g compost (moisture content 75%, w/w) to mimic the average bulk density in the tunnel of 540 kg $m^{-3}$. Compost temperature was monitored

with a thermistor. The self-heating of the compost samples made it difficult to maintain a constant temperature. In order to reduce the effect of differences in compost fiber orientation, measurements at a given temperature were done in triplo, starting with (re)positioning the lambda needle. Measurements were conducted for straw compost and horse manure compost at 5 °C intervals in a temperature range from 20 to 70 °C.

*Separate measurement of compost and air temperature.* During filling of the containers, small plastic cylindrical cages (1.9 × 8.5 cm, r × L; 0.8 x 3 cm mazes) were placed at 40, 120 and 160 cm height from the bottom, three on each level. Care was taken to remain them empty of compost. Every cage contained two thermistors to measure the air temperature. Compost temperature was measured on two spots close to the cage by twisting a tuft of substrate firmly around a thermistor. Temperatures were recorded every 30 min during 7 days with thermistors and a recorder (Kipp & Zonen BD121, accuracy 0.2 °C). Three moisture samples were taken around each cage after 7 days.

*Computer equipment and software*

A combination of FORTRAN and the Continuous Simulation Modeling Program (CSMP) (Speckhart & Green, 1976) was used on a DEC MicroVax II computer (8 Mbyte memory; two 70 Mb disks). The technique used was Time-Dependent Analysis (Moretti & Abbett, 1966). Numerical integration was accomplished according to a 4th-order Runge Kutta approximation. CPU time for a simulation run was 8 h.

## Results

*Parameters, equations and data*

The contribution of diffusion and natural convection to mass and energy transport in compost is negligible with respect to the contribution by forced convection because of the high air velocity of 0.1 m $s^{-1}$ in the pores (Beukema *et al.*, 1982). Since the walls of tunnels are insulated and impervious, transport processes are assumed to occur only along the air flow path in vertical direction. Temperature measurements in a horizontal plane support this assumption. Hence, a one dimensional description of the tunnel process is chosen (Gray *et al.*, 1971; Lentz *et al.*, 1971).

Compost is considered as a porous medium consisting of a compost phase and a gas phase. The compost phase, consisting of solids and water, is treated as one phase with solid-like behaviour. Water transport is considered to occur only as vapour transport in the gas phase.

The physical composition of compost is characterized by moisture content $\chi$, bulk density $\rho_c$ and porosity $\varepsilon$. The moisture content $\chi$ is defined as the difference between total weight $m_t$ and dry weight $m_d$ divided by total weight:

$$\chi = \frac{m_t - m_d}{m_t} \text{ [–]} \quad (1)$$

Bulk density $\rho_c$ is formulated as:

$$\rho_c = \frac{m_t}{V_t} \text{ [kg m}^{-3}\text{]} \quad (2)$$

Porosity $\varepsilon$ is defined as the volume $V_a$ occupied by the gas phase divided by the total volume $V_t$:

$$\varepsilon = \frac{V_a}{V_t} = 1 - \frac{V_d + V_w}{V_t} \text{ [–]} \quad (3)$$

From the density $\rho_c$ and the moisture content $\chi$, the porosity $\varepsilon$ can be expressed as:

$$\varepsilon = 1 - \left( \chi \cdot \frac{\rho_c}{\gamma_w} + (1-\chi) \cdot \frac{\rho_c}{\gamma_d} \right) \text{ [–]} \quad (4)$$

where $\gamma_w$, the specific density of water, is 1000 kg m$^{-3}$ (Krischer & Esdorn, 1956), and $\gamma_d$, the specific density of organic material, is 1500 kg m$^{-3}$ (Ohm, 1972).

Compost is compressible and exhibits both elastic and plastic behaviour (Randle & Flegg, 1985). During composting also subsidence occurs. Therefore, bulk density and porosity vary with height and time.

Experimental data on dry matter and moisture are given in Table 1. Extensive temperature monitoring in a horizontal plane perpendicular on the direction of the air stream revealed only differences less than 1 °C. Visual inspection of the compost in the containers revealed a wet top layer of the substrate as a result of dripping of condensated water from the roof of the tunnel.

In containers in tunnels, the filling heights varied from 172–181 cm. The initial thickness of layers of compost of 100 kg varied from 14.8 cm in the bottom section of the container to 20.6 cm in the top section (SD = 0.3, $n$ = 30). Density measurements and corresponding calculated porosity data for composts are presented in Figure 2. Mean initial density and porosity values were put in a table and used as input for the model equations. The dry matter and moisture contents for two trials are given in Table 2. A moisture gradient exists in the direction of the air stream. Other trials revealed identical gradients in the moisture content. The low moisture content in the bottom part in combination with the lower dry matter loss in that section suggests retarded biological activity.

Table 1. Average process characteristics for a container in a tunnel during Phase II composting, based on 10 trials. Average air flow was 150 m$^3$ tonne$^{-1}$ h$^{-1}$.

| | Start | End |
|---|---|---|
| Total | 1000 kg | 730 kg |
| Water | 750 kg | 518 kg |
| Dry matter | 250 kg | 212 kg |
| Void volume | 50% | 60% |

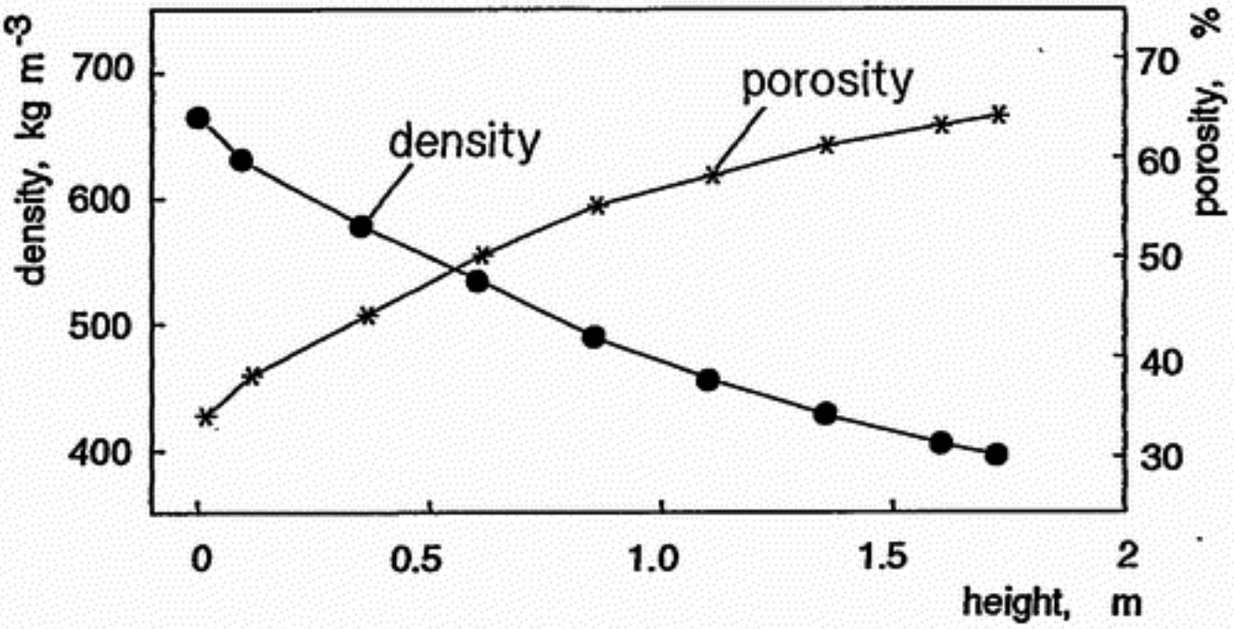


Figure 2. Average density and calculated porosity for compost in a container; filling weight 1000 kg (930 kg $m^{-2}$). Moisture content is 74.6% (w/w; $n = 6$).

The compost settles slowly in opposite direction to the air flow and the volume of the compost changes as a result of degradation and evaporation. A material coordinate system must be introduced to describe such a dynamic system. This coordinate system is attached to the compost phase and subsides with constant velocity. However, this will lead to complicated mathematical formulations of transport processes. To avoid these difficulties a stationary coordinate system is used instead of material coordinates. Hence, to describe transport processes, compost is considered as rigid whereas for the calculation of porosity and bulk density compost is considered as non-rigid. This calculation procedure introduces errors in the heat and

Table 2. Calculated weights of water and dry matter (DM) from measured moisture contents and layer weights (triplo) of ten layers in a container after completion of Phase II (trials 1371 and 1376). The initial weight of each layer was 100 kg (76 kg water and 24 kg DM), average air recirculation rate was 150 $m^3$ tonne $h^{-1}$.

| Layer | Water kg | Dry matter kg | Moisture % |
|---|---|---|---|
| (top) | | | |
| 1 | 49.0 | 20.0 | 71.0 |
| 2 | 47.1 | 20.1 | 70.1 |
| 3 | 45.0 | 19.8 | 69.4 |
| 4 | 44.1 | 20.0 | 68.8 |
| 5 | 43.2 | 20.0 | 68.4 |
| 6 | 41.8 | 19.9 | 67.7 |
| 7 | 40.9 | 20.2 | 66.9 |
| 8 | 40.1 | 20.1 | 66.6 |
| 9 | 37.1 | 21.1 | 63.7 |
| 10 (bottom) | 21.0 | 23.5 | 47.2 |

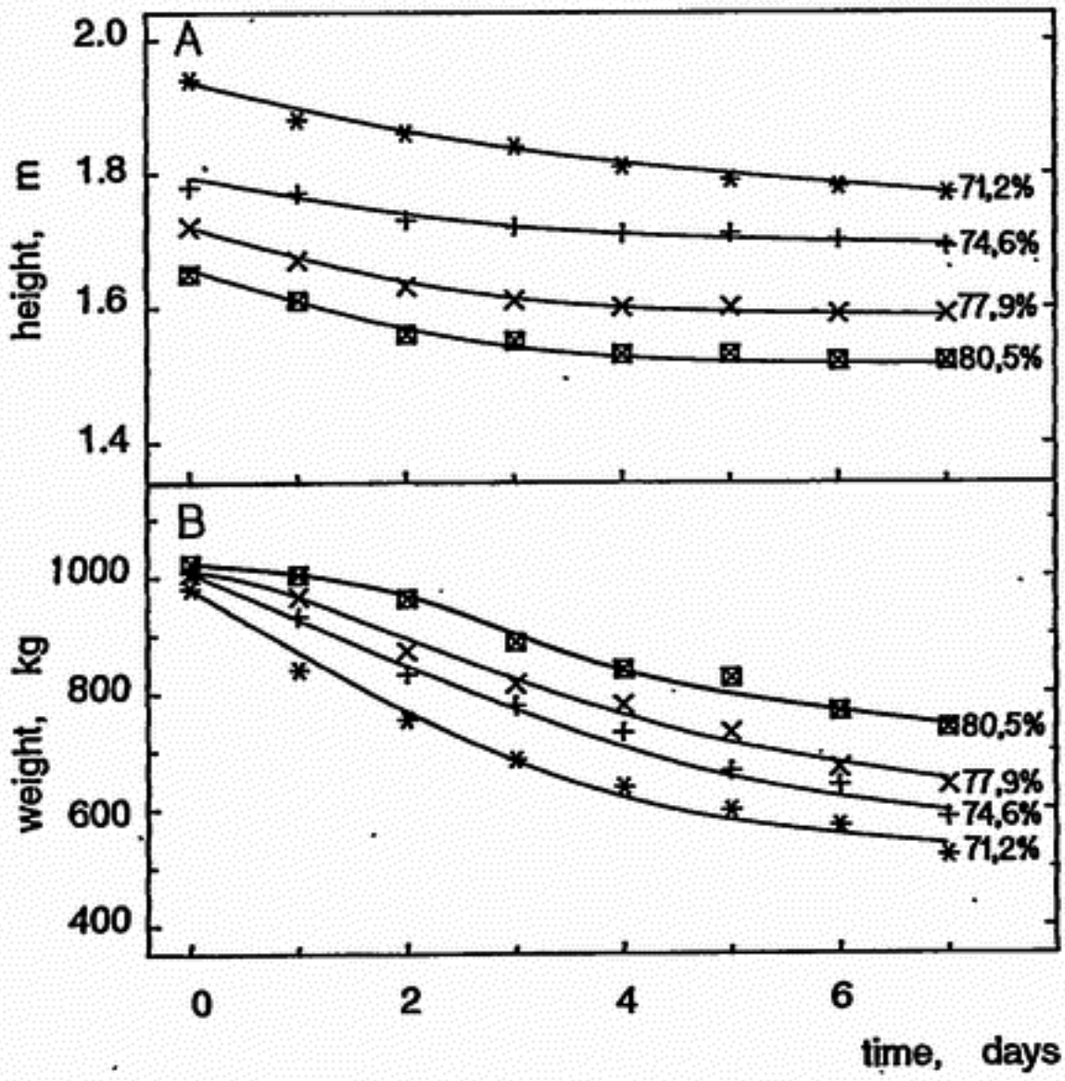


Figure 3. Reduction in height (A) and weight (B) for compost with moisture contents as indicated (trial 1447). The curves in A were obtained using equation 6. In B, for $\chi$ of 71.2 and 74.6% (w/w), equation 5 was used; for $\chi$ of 77.9 and 80.5 a polynomial regression was used.

mass balances. Fortunately, these errors are negligible because forced convection strongly dominates local velocities of the settling compost.

Experimental data on the decrease in height and weight are shown in Figure 3. The curves for $\chi$ of 71.2 and 74.6% in Figure 3B are obtained by using equation 5:

$$m_t = m_o \cdot 10^{(a-b\chi)\cdot t} \text{ [kg]} \qquad (5)$$

where $m_0$ is initial weight [kg], $\chi$ is the initial moisture content, $t$ is the process time, $a = 0.0338$ and $b = 0.07$ respectively (correlation coefficient 0.93). For $\chi$ of 77.9 and 80.5% a polynomial regression was used for better fitting. Measurements in the two latter cases showed an increased pressure difference over the compost layers, probably due to a percolate water film in the bottom of the containers. At higher moisture contents we observed increased loss of percolate water. The normal loss is 23 kg tonne$^{-1}$ but at 77.9 and 80.5% this was 26 and 30 kg tonne$^{-1}$, respectively. Dry matter reduction rate and height reduction rate were similar at all four moisture levels. From the data we deduced a relation between height and time:

$$h_t = h_o \cdot 10^{(a_1 - a_2\chi)\cdot t} \text{ [m]} \quad (6)$$

in which $h_0$ is the initial height, $\chi$ is the moisture content, $t$ is the time, $a_1 = 0.0324$ d$^{-1}$ and $a_2 = 0.07$ d$^{-1}$ (correlation coefficient 0.91).

The biological decomposition of organic matter is assumed to be the aerobic degradation of cellulose (Alexander, 1977) according to the overall equation:

$$(C_6H_{10}O_5)_n + 6\,O_2 \rightarrow (C_6H_{10}O_5)_{n-1} + 6\,CO_2 + 5\,H_2O \quad (7)$$
$$\Delta H^0 = -2834.6 \text{ [kJ mol}^{-1}\text{]}$$
$$= -17498 \text{ [kJ kg}^{-1}\text{]}$$

Kuter *et al.* (1985) studied the effects of aeration and temperature on composting of municipal sludge in a vessel system. From measured losses of water and solids and from $CO_2$ evolution they conclude that aerobic degradation of glucose is a major source of energy production. Hemicellulose is also important (Gerrits *et al.*, 1967), its degradation being similar. Equation 7 gives no information about the rate at which degradation takes place. Lomax *et al.* (1984) showed that microbial degradation, and thus heat production rate $W$, depends on temperature $T$ and the state of decomposition at time $t$.

Data on dry matter conversion from trial 1447 (Figure 4A) were used to calculate the heat production $W$ (Figure 4B). In the first two days maximal values are reached. Most likely, more easily degradable nutrients such as soluble carbohydrates, hemicellulose and proteins will degrade before high molecular weight cellulose is converted. The moisture content of the substrate had no detectable influence on the value of the heat production because the dry matter reduction rate was not affected. This implies that the small variation in porosity has no detectable influence on the value of $W$ either. The ratio of water loss to dry matter loss was constant at 6.2 kg kg$^{-1}$ ($n = 8$, SD = 0.6). Numerical values of $W(T,t)$ are stored in the computer model. These values and equation 7 are used as a starting point to model rates of dry matter losses and biological production of water and carbon dioxide.

Carbon dioxide and oxygen concentration were measured in the bottom and top section of the tunnel. Carbon dioxide production of compost was calculated from the consumption of dry matter. Combined with the average flow rate of process air, the carbon dioxide concentration in the top section of the tunnel should be 0.2% higher than in the bottom section. This was consistent with actual measurements.

The volumetric dry matter content $\rho_d$ changes as a result of degradation but also by compaction (e.g. settlement) of the compost. Therefore, changes of $\rho_d$ with respect to time are given by:

$$\frac{\partial \rho_d}{\partial t} = -5.7 \cdot 10^{-8} \cdot W(T,t) \cdot \rho_c - \frac{\rho_d}{V_t} \cdot \frac{dV_t}{dt} \text{ [kg m}^{-3}\text{ s}^{-1}\text{]} \quad (8)$$

In equation 8 the first term on the right hand side accounts for the degradation processes. The second term accounts for compaction. In a one dimensional model the total volume $V_t$ per unit pile length is equal to height $h$. Then, from equation 6 it follows:

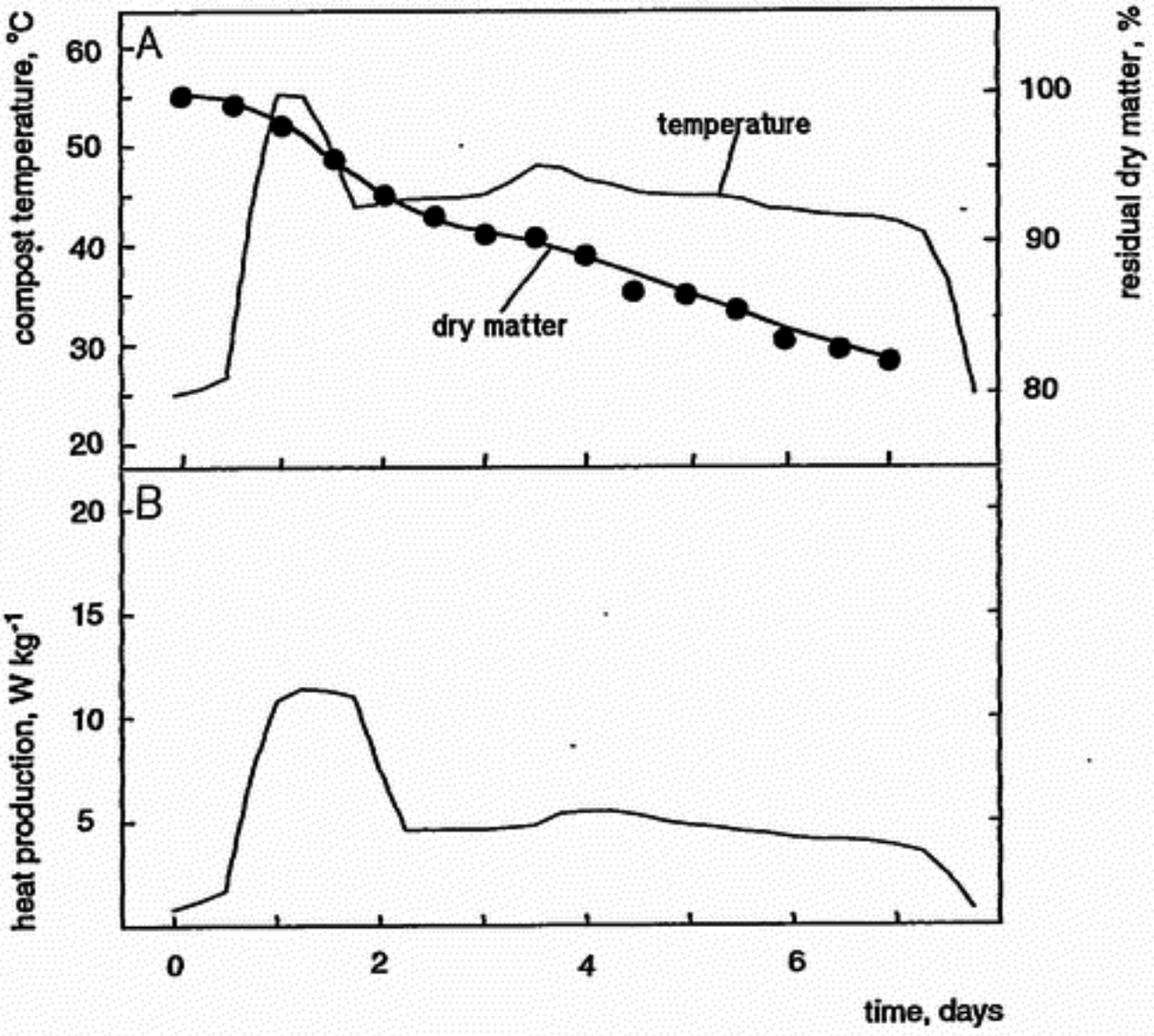


Figure 4. A. Temperature and reduction of dry matter during composting (trial 1447). The curve of residual dry matter is a fitted polynomial. B. Calculated heat production from dry matter conversion data and temperature. The data are valid for moisture contents between 71 and 80% (w/w) at the beginning of composting.

$$\frac{dV_t}{dt} = \frac{dh}{dt} = (a_1 - a_2\chi) \cdot h_o \cdot 10^{(a_1 - a_2\chi)\cdot t} \quad [\mathrm{m\ s^{-1}}] \tag{9}$$

Combining equations 8 and 9 leads to:

$$\frac{\partial \rho_d}{\partial t} = -5.7 \cdot 10^{-8} \cdot W(T,t) \cdot \rho_c - (a_1 - a_2\chi) \cdot \rho_d \quad [\mathrm{kg\ m^{-3}\ s^{-1}}] \tag{10}$$

The rate at which the volumetric water content changes, depends on microbial activity and compaction, but also on the rate of evaporation $R_w$ (given in equation 16). Hence it is given by:

$$\frac{\partial \rho_w}{\partial_t} = -3.2 \cdot 10^{-8} \cdot W(T,t) \cdot \rho_c - (a_1 - a_2 \cdot \chi) \cdot \rho_w - R_w \quad [\mathrm{kg\ m^{-3}\ s^{-1}}] \tag{11}$$

The concentration of water in the gas phase is determined by the water vapour bal-

ance which expresses the principle of conservation of water vapour in a infinitesimal volume. The rate of change of water vapour is equal to the sum of the net vapour transport by convection and diffusion and the amount of evaporation:

$$\frac{\partial(\varepsilon \cdot C_w)}{\partial t} = -v \cdot \frac{\partial C_w}{\partial z} \cdot + \frac{\varepsilon}{\beta^2} \cdot D_w \cdot \frac{\partial^2 C_w}{\partial z^2} + R_w \quad [\text{kg m}^{-3}\,\text{s}^{-1}] \tag{12}$$

where $C_w$ is the water vapour concentration in the gas phase, $v$ is the superficial velocity defined as the volume flow rate divided by the area of a plane perpendicular to the flow direction, $z$ is the vertical coordinate, $\beta$ is the tortuosity which accounts for the tortuous stream line of fluid flow in the porous medium. We estimate $\beta = 0.91$. Since vapour transport by diffusion is of minor importance in comparison with convective transport, the porosity is set at a constant value of 0.5 only in the second term of equation 12. $D_w$ is the coefficient of diffusion of water vapour in air. At atmospheric pressure it is estimated by:

$$D_w = 0.23 \cdot 10^{-4} \cdot \left(1 + \frac{T}{273.15}\right)^{2.3} \quad [\text{m}^2\,\text{s}^{-1}] \tag{13}$$

(Krischer & Esdorn, 1956) in which $T$ is the actual compost temperature ( °C). It is assumed that the gas phase is saturated with water vapour at prevailing temperatures.

The saturated water vapour concentration in the gas phase depends on $T$ and is given by:

$$C_w = \frac{b_1 \cdot M \cdot e^{\left(\frac{-b_2}{R \cdot (T+273.15)}\right)}}{R \cdot (T+273.15)} \quad [\text{kg m}^{-3}] \tag{14}$$

(Ohm, 1972), where $M$ is the molecular weigth of water, equal to 18 kg kmol$^{-1}$, $R$ is the universal gas constant equal to 8310 J kmol$^{-1}$ K$^{-1}$, and $b_1$ and $b_2$ are equal to 1.375 $10^{11}$ J m$^{-3}$ and 4.356 $10^4$ J kmol$^{-1}$, respectively (Ohm, 1972). As $C_w$ depends on $T$, and $\varepsilon$ depends on time, the first term in equation 12 becomes:

$$\frac{\partial(\varepsilon \cdot C_w)}{\partial t} = \varepsilon \cdot \frac{dC_w}{dT} \cdot \frac{\partial T}{\partial t} + C_w \cdot \frac{\partial \varepsilon}{\partial t} \quad [\text{kg m}^{-3}\,\text{s}^{-1}] \tag{15}$$

Combination of equations 12 and 15 gives:

$$R_w = \varepsilon \cdot \frac{dC_w}{dT} \cdot \frac{\partial T}{\partial t} + C_w \cdot \frac{\partial \varepsilon}{\partial t} + v \cdot \frac{\partial C_w}{\partial z} - \frac{\varepsilon}{\beta^2} \cdot D_w \cdot \frac{\partial^2 C_w}{\partial z^2} \quad [\text{kg m}^{-3}\,\text{s}^{-1}] \tag{16}$$

Equation 16 states that the rate of evaporation is the matching factor between changes of saturated vapour pressure and net vapour transport. The first term on the right hand side of equation 16 expresses the effect of temperature changes and is obtained by differentiation of equation 14 to $T$:

$$\frac{\partial C_w}{\partial T} = \frac{b_1 \cdot M \cdot e^{\left(\frac{-b_2}{R \cdot (T+273.15)}\right)} \cdot \left(\frac{-b_2}{R \cdot (T+273.15)} - 1\right)}{R \cdot (T+273.15)^2} \quad [\text{kg m}^{-3}\,\text{s}^{-1}] \tag{17}$$

The second term in equation 16 accounts for changes of porosity. As $V_d / V_t = \rho_d / \gamma_d$ and $V_w / V_t = \rho_w / \gamma_w$, the following expression for $\varepsilon$ is deduced from equation 3:

$$\varepsilon = 1 - \left( \frac{\rho_d}{\gamma_d} + \frac{\rho_w}{\gamma_w} \right) \quad [-] \tag{18}$$

Differentiation with respect to t gives:

$$\frac{\partial \varepsilon}{\partial t} = 1 - \left( \frac{1}{\gamma_d} \cdot \frac{\partial \rho_d}{\partial t} + \frac{1}{\gamma_w} \cdot \frac{\partial \rho_w}{\partial t} \right) \quad [s^{-1}] \tag{19}$$

Changes in porosity can now be calculated by inserting equations 10 and 11 into 19. For the specific density of dry matter we used $\gamma_d = 1500$ kg m$^{-3}$ (Ohm, 1972) and for the specific density of water $\gamma_w = 1000$ kg m$^{-3}$ (Krischer & Esdorn, 1956).

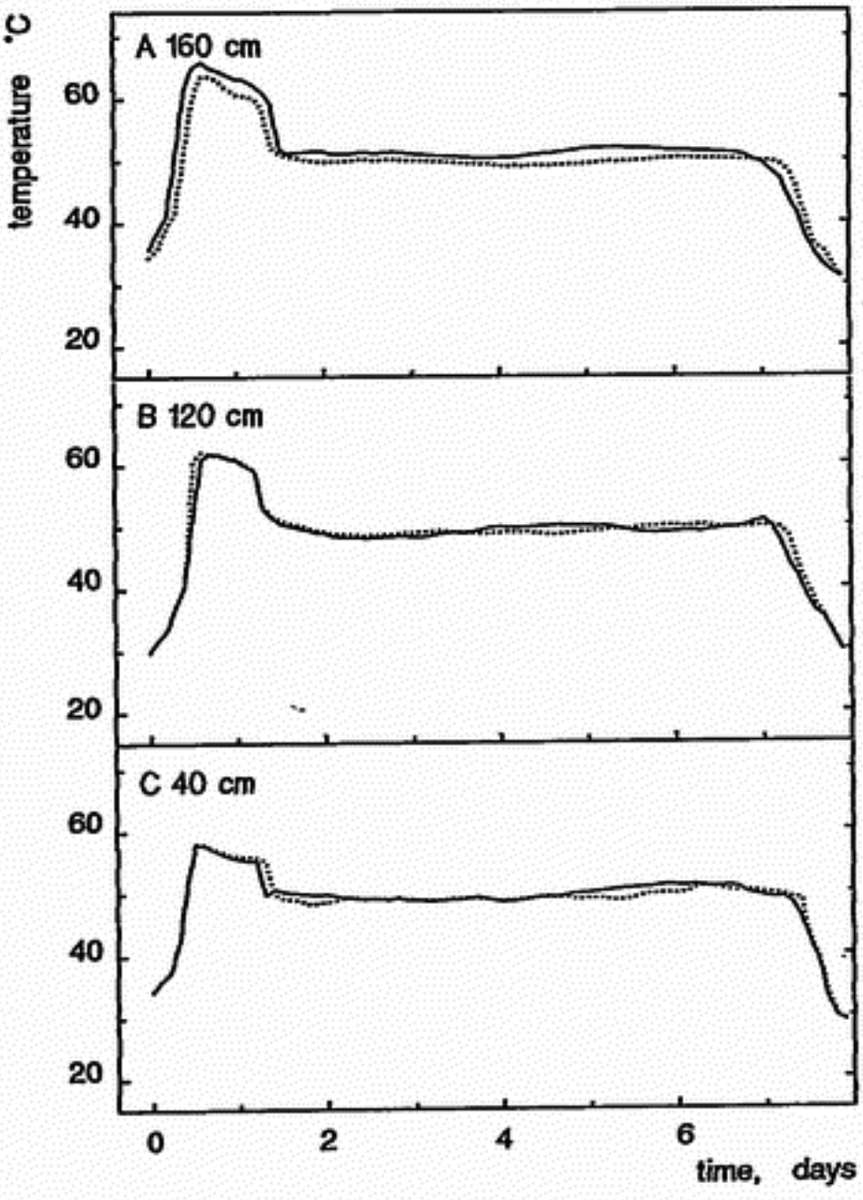


Figure 5. Average air and compost temperatures in the bulk of horse manure compost (moisture content 73.5%). A, at 160 cm; B, at 120 cm; C, at 40 cm height from the bottom. Horse manure compost was used with a moisture content of 75%, an substrate density of 540 kg m$^{-3}$, and a total height 178 cm.

Separate measurements of compost and air temperatures in the substrate are presented in Figure 5. Trials with straw and horse manure compost gave similar results. The results reveal differences between air and compost temperatures in the bulk. At 40, 120 and 160 cm height different temperature patterns exist. The bottom layer (Figure 5C), closest to the entrance of colder recirculated process air, is coolest. In the top layer (Figure 5A) the air temperature is significantly higher than the compost temperature probably as a result of the observed extra condensation in this area.

However, the observed minor differences in temperature are not relevant for calculations and are ignored for simplicity: in the model equal temperatures are assumed for the compost and the gas phase.

The temperature of compost is determined by the heat balance. The rate of accumulation of internal energy is equal to the sum of the net rate of heat transfer and heat production. Heat transfer takes place by convection and conduction and transport of latent heat ($H \cdot R_w$; $H$, the heat of evaporation of water at existing temperature (see equation 22); $R_w$, the rate of evaporation [kg $m^{-3}$ $s^{-1}$]). In mathematical form the heat balance is written as:

$$(\rho_c \cdot c_{p,c} + \varepsilon \cdot \gamma_a \cdot c_{p,a}) \cdot \frac{\partial T}{\partial t} =$$

$$= -\gamma_a \cdot c_{p,a} \cdot v \cdot \frac{\partial T}{\partial z} + \lambda \cdot \frac{\partial^2 T}{\partial z^2} - A \cdot \frac{K}{\delta} \cdot (T - T_0) - H \cdot R_w + W(T,t) \cdot \rho_c \quad [J\,m^{-3}\,s^{-1}] \quad (20)$$

in which $\gamma$ stands for the density, $\rho_p$ for specific heat at constant pressure, subscripts $c$ and $a$ respectively for the compost phase and the gas phase, $\varepsilon$ for porosity, $T$ for compost temperature, $T_o$ for ambient temperature, $t$ for time, $\lambda$ for the thermal conductivity of compost, $A$ for the area of the enclosing wall, $K$ for the thermal conductivity of the tunnel wall of polyurethane foam, $K = 0.04$ $W\,m^{-1}\,K^{-1}$, $\delta$ for the thickness of the wall, $H$ for the heat of evaporation, $R_w$ for the rate of evaporating water and $W$ for the rate of microbial heat production.

The specific heat of the compost phase is computed as:

$$c_{p,c} = (1 - \chi) \cdot c_{p,d} + \chi \cdot c_{p,w} \quad [J\,kg^{-1}\,K^{-1}] \quad (21)$$

in which subscripts $d$ and $w$ indicate solids and water respectively and $\chi$ is the moisture content. For $c_{p,d}$ we adopt a value of 1220 J $kg^{-1}$ $K^{-1}$ (Ohm, 1972) and for $c_{p,w}$ a value of 4180 J $kg^{-1}$ $K^{-1}$ (Krischer & Esdorn, 1956). For $c_{p,a}$ of moist air a temperature dependent table (Krischer & Esdorn, 1956) is used in the model.

The heat of evaporation depends on temperature and is calculated by:

$$H = 2.38 \cdot 10^6 + 1820 \cdot T \quad [J\,kg^{-1}] \quad (22)$$

with $T$ (°C).

The thermal conductivity of compost as a function of temperature (Figure 5) was derived from experimental data (estimated accuracy of 0.05 W $m^{-1}$ $K^{-1}$):

$$\gamma = 3.3 \cdot 10^{-4} \cdot T^2 - 0.015 \cdot T + 0.421 \quad [W\,m^{-1}\,K^{-1}] \quad (23)$$

with $T$ (°C). Equation 23 is valid for compost temperatures between 20 and 70 °C.

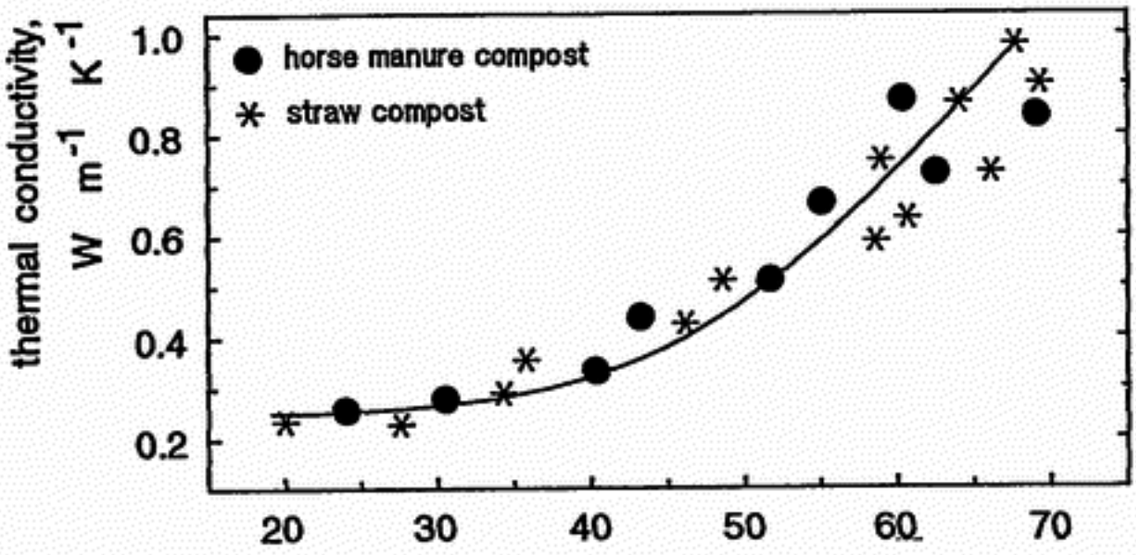


Figure 6. Thermal conductivity data of straw (*) and horse manure (.) composts as a function of temperature. The curve was obtained using equation 23.

Oxygen is transported by convection and diffusion and is consumed as a result of microbial activity. The oxygen concentration $C_{ox}$ depends on the oxygen balance, which is written similar to equation 12:

$$\frac{\partial(\varepsilon \cdot C_{ox})}{\partial t} = \varepsilon \cdot \frac{\partial C_{ox}}{\partial t} + C_{ox} \cdot \frac{\partial \varepsilon}{\partial t} =$$

$$= -v \cdot \frac{\partial C_{ox}}{\partial z} + \frac{\varepsilon}{\beta^2} \cdot D_{ox} \cdot \frac{\partial^2 C_{ox}}{\partial z^2} + R_{ox} \quad [\text{kg m}^{-3}\,\text{s}^{-1}] \tag{24}$$

where $D_{ox}$ is the binary coefficient of diffusion of oxygen in air. $D_{ox}$ is assumed to be independent of temperature and is estimated as $1.33\ 10^{-5}$ m$^2$ s$^{-1}$ (Krischer & Esdorn, 1956). $R_{ox}$, the oxygen consumption rate, follows from equation 7:

$$R_{ox} = -6.8 \cdot 10^{-8} \cdot W(T,t) \cdot \rho_c \quad [\text{kg m}^{-3}\,\text{s}^{-1}] \tag{25}$$

Since oxygen consumption is related to carbon dioxide production by a 1:1 stoichiometric ratio (Schisler, 1982) and the coefficient of diffusion of both gases has approximately the same value, the carbon dioxide concentration is estimated as the difference between the ambient oxygen concentration, i.e. 21 vol%, and the local oxygen concentration. It is therefore not necessary to set up a separate differential equation for the carbon dioxide balance.

*Numerical formulation*

The partial differential equations (PDE) 16, 20, and 24 are non-linear and coupled. Therefore, a numerical method is employed to solve these equations. The numerical solution starts with the discretization concept in which the continuous information contained in the exact solution of the PDE is replaced by discrete values at certain grid points contained in the discretization equation (Lapidus & Pinder, 1982). For our model this means that the compost pile is divided in 10 layers of equal thickness.

Each grid point is located in the center of a layer.

The discretization equation can be derived in many ways. In this model the finit difference method (FDM) is used (Lapidus & Pinder, 1982). This method uses central differences, obtained from truncated Taylor series expansions, to approximate derivatives in the differential equation. The central difference scheme assumes that the dependent variable, e.g. $T$, at the interface between two adjacent layers can be calculated by linear interpolation between the grid point values. Unfortunately, in case of forced convection, this scheme can give physical unrealistic results and may lead to numerical instabilities. At high velocities, $T$ at the interface is dominated by the upstream value. Then the upwind scheme is a better alternative. This scheme uses the upstream value of $T$ in the convective term and the central difference approach for the diffusive or conductive term. In order to decide whether the upwind scheme or the central difference scheme must be employed, the layer Péclet number is introduced:

$$Pé = \frac{v \cdot \Delta z}{D} \quad [-] \tag{26}$$

where $Pé$ is the Péclet number, $\Delta z$ is the distance between two adjacent grid points and $D$ is the coefficient of diffusion. In case of heat transfer $D = \lambda / (\rho c_p)$. If the absolute value of the Péclet number is less than or equal to 2, the central difference scheme is used. In all other cases the upwind scheme is recommended. In the tunnel system air velocity is equal to 0.1 m $s^{-1}$, $\Delta z$ is 0.1 m and $D$ has an order of magnitude of $10^{-5}$ $m^2$ $s^{-1}$. Thus, the layer Péclet number approaches 1000 and the upwind scheme is used.

*Initial and boundary conditions*

Ambient conditions are used as initial conditions for temperature and oxygen fields. The saturated water vapour concentration at ambient temperature holds as initial condition for the vapour field. Real process data are used as initial conditions for bulk density, porosity, dry weight and moisture content. The temperature of the return air in the bottom of the tunnel is calculated from the amount, temperature and relative humidity of supplied fresh air and the amount of recirculated air. The temperature and relative humidity of the recirculated air are calculated. A correction for heat loss during recirculation of 5% is implemented. For comparison with the model calculations, the temperature of the return air is also measured.

The conductive heat transfer from top (equation 27) and bottom layers (equation 28) to the environment are expressed by:

$$q_{top} = \frac{\lambda_1 \cdot \alpha_x \cdot (T_x - T_1)}{2 \cdot \Delta z} \quad [\mathrm{W\ m^{-2}}] \tag{27}$$

$$q_{bot} = \frac{\lambda_{n+1} \cdot \alpha_y \cdot (T_n - T_y)}{2 \cdot \Delta z} \quad [\mathrm{W\ m^{-2}}] \tag{28}$$

where $q_{top}$ and $q_{bot}$ are the conductive heat fluxes from top and bottom layers respectively, $\lambda_1$ and $\lambda_n$ are the thermal conductivities of the top and bottom layers, $\alpha_x$ and

$\alpha_y$ are transfer coefficients between compost layers and air at top and bottom section. $T_x$ is the air temperature at the top, $T_y$ is the air temperature at the bottom, $T_1$ and $T_n$ are the compost temperatures of top and bottom layers respectively and $\Delta z$ is the distance between two adjacent grid points. From 6 trials we obtained values for $\alpha_x$ and $\alpha_y$ close to 0.5, being used in the calculations.

For the convective heat transfer the boundary conditions are:

$$f_{top} = -v \cdot \rho_a \cdot c_{p,a} \cdot 0.5 \cdot (T_x + T_1) \quad [\text{W m}^{-2}] \tag{29}$$

$$f_{bot} = -v \cdot \rho_a \cdot c_{p,a} \cdot 0.5 \cdot (T_y + T_n) \quad [\text{W m}^{-2}] \tag{30}$$

The superficial velocity of air should be in the range of 0.01–0.11 m $s^{-1}$. The boundary conditions for oxygen and water vapour fields are formulated in a similar way, i.e. $T_x$ is replaced by $C_{w,x}$ or $C_{ox,x}$.

*Overview of input and output data*

The input in the program consists of the initial temperatures of compost and air, the amount of supplied fresh air and its relative humidity, and the amount of recirculated air. Also the initial weight, moisture content and filling height of compost are input data. The following data are stored in the program: heat production and thermal conductivity of compost as a function of filling height, and settling related to process time.

Output data are the time-course of the main conductive and convective heat and mass flows and, from this, an overall process balance. Also continuous data on temperature, oxygen and carbon dioxide concentration, dry matter and moisture content, and mass and height for every layer are calculated.

*Comparison of actual and calculated data*

Calculated parameter-time curves were compared with actual process data. As an example we present trial 1415 (moisture content 75%). The process time was 7.5 days. The actual and calculated results for one tunnel container filled with 1000 kg fresh substrate are shown in Figure 7. The actual fresh and total supply air rates are depicted in Figure 7A. Actual and calculated compost temperatures were very similar (Figure 7B). By comparison of Figs. 7A and 7B, it is evident that the desired pasteurization temperature was reached only by diminishing the amount of supply air. Due to the high biological activity of the substrate during the first 3 days, extra supply air was needed. Figure 7C depicts the temperatures of the supply and return air, below and above the substrate respectively. Comparison of Figures 7B and 7C shows that the air temperature in bottom and top section of the tunnel were different from the compost temperature and sensitive to changes in activity of the substrate.

Figures 7D and 7E show the change in weight and height of the compost in the container. Usually, measured weight losses during the first day are the highest due to higher activity. During the course of the process up to 30% settling of the compost

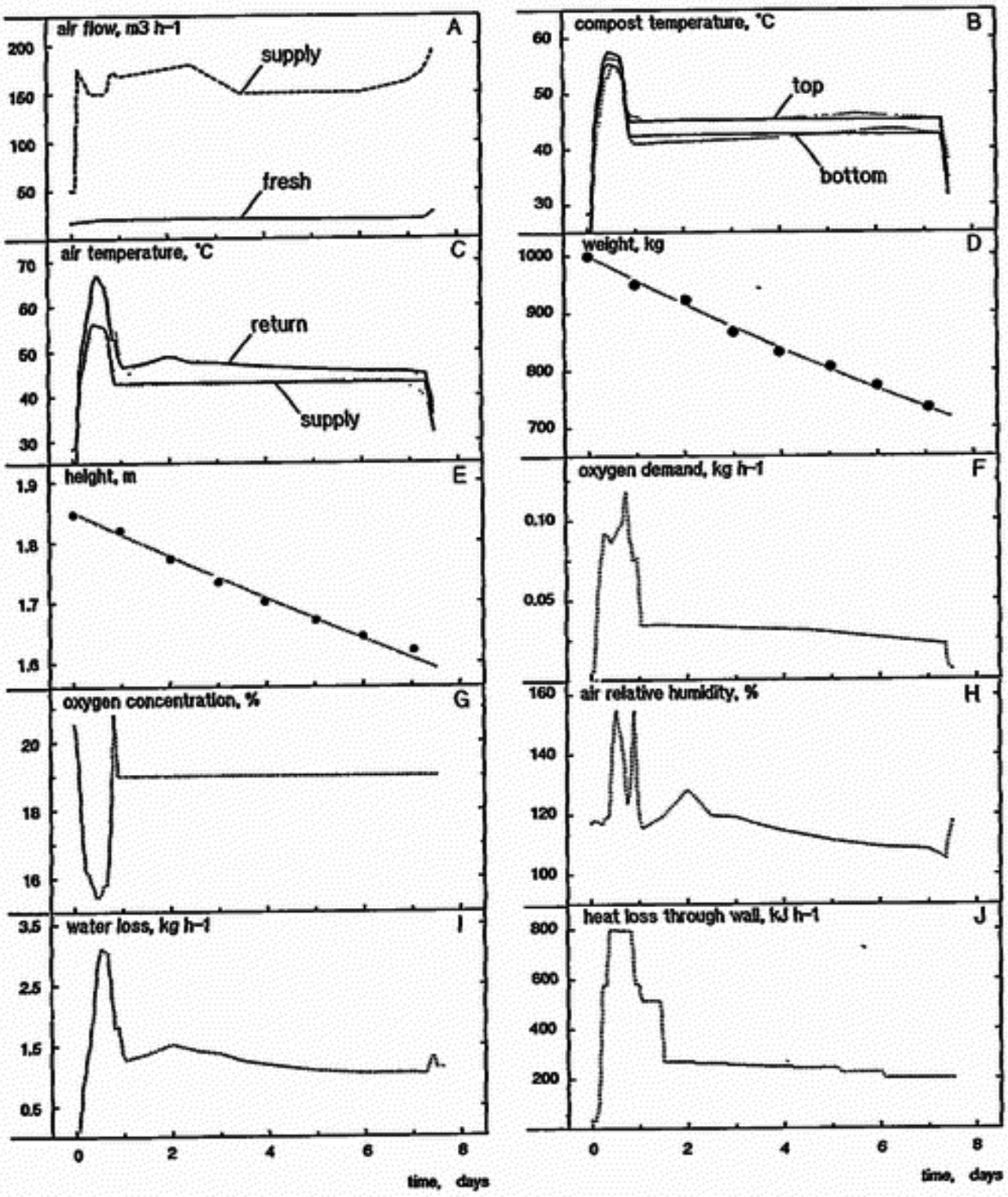


Figure 7. Actual and calculated process values (trial 1415) during Phase II composting for a container filled with 1000 kg (moisture content 75%). The process time [d] is depicted on the horizontal axis.
A: Actual amount of fresh air (—) and supply air (—); B: Actual (—) and calculated (—) substrate temperatures in bottom and top layer; C: Actual (—) and calculated (—) temperatures of supply and return air, below and above the substrate respectively; D: Actual (.) and calculated (—) bulk weight of compost; E: Actual (.) and calculated (—) height of compost; F: Calculated $O_2$ demand of the substrate; G: Calculated $O_2$ concentration in the return air in the top section; H: Calculated relative humidity of the supply air in the bottom section; I: Calculated water loss of the compost; J: Calculated heat loss through the walls of the container.

was observed. Considering the reduction in mass, the actual stream of supply air can reach 230 $m^3$ $tonne^{-1}$ $h^{-1}$. Both the calculated $O_2$ demand (Figure 7F) and the concentration of $O_2$ in the process air in the top section of the container (Figure 7G) reflect the peak activity of the substrate during the pasteurization period. The calculated average $O_2$ consumption rate was used to calculate the total dry matter loss during the process and showed good agreement with actual data. The measured $O_2$ concentration in the return ducts show a similar pattern as Figure 7G. During pasteurization the average $O_2$ concentration was about 15%; later during conditioning it was 19%. After mixing of fresh air with return air, the supply air can be oversaturated with water vapour (Figure 7H; confirmed by air sampling in the bottom of tunnels). Most likely this will lead to extra condensation of water in the supply ducts. Figure 7I depicts the calculated water loss. The total water loss as derived from Figure 7I showed a maximum deviation of 6% from the calculated overall water loss according to moisture and weight data. Figure 7J shows the calculated heat loss through the wall. An important factor which accounts for the maximum in water loss during pasteurization is the exponential relation of the potential water vapour content of air to the temperature. The calculated overall water loss closely resembled the experimentally determined value from moisture data of the compost. We further observed an average loss of percolate water of $23 \pm 2$ kg $tonne^{-1}$ substrate ($n = 10$). This value was incorporated in the overall balance sheet calculation in the model. About 14% of the total generated heat was discharged as conductive heat.

## Discussion

Considering the good agreement between calculated and actual process results (Figure 7), we conclude that the concepts expressed in the model equations are decisive for the physico-chemistry of compost preparation for mushroom cultivation.

During the process fresh air at 20 $m^3$ $tonne^{-1}$ $h^{-1}$ (15% of total air flow) is needed to remove excess heat, while only 1.9 $m^3$ $tonne^{-1}$ $h^{-1}$ is needed to supply $O_2$. Thus most of the convective air is needed to control temperature and not to supply $O_2$. This was also concluded on basis of overall calculations (Randle, 1977). $O_2$ or $CO_2$ controls for process management may be useful only at the start of the process when temperature is allowed to increase for pasteurization. Calculations on dry matter loss via $CO_2$ production measurements are consistent with temperature based calculations.

Diffusion of energy and mass is small compared to convection, mainly as a result of the high air velocities in the system. On average 70% of the total heat produced is discharged as latent heat, 12% is used for heating the compost and process air, 14% is lost through the walls by conduction and another 4% is lost through condensation in the air ducts and return channels. Convection of heat is more important than conduction, in agreement with Hogan *et al.* (1989). The loss of heat through the walls will even be of less significance in large commercial tunnels, particularly when tunnels are placed in series.

Water losses increase at higher supply air rates and higher process temperatures

(Gerrits, 1982). In particular the bottom section is vulnerable to desiccation, resulting in a poor quality compost in that section. Air circulation rates below 100 $m^3$ $tonne^{-1}$ $h^{-1}$ lead to lower water losses but at the same time to an untolerable large temperature gradient in the substrate, which reduces the quality of the compost. Therefore, we prefer to regulate the process on temperature, controlled by means of ventilative heat management.

The model ingnores the influence of nitrogen on composting. The moment when the concentration of volatile $NH_3$ is below 10 ppm, *i.e.* when composting is completed, not being calculated. Also the effect of nitrogen on the heat production is not accounted for. Recently we found that compost with chicken manure was more active than compost without; the heat productions were 5.3 and 3.9 W $kg^{-1}$ dry matter respectively (unpublished). This effect might be expressed as a factor in the equation for the heat production and supports the need for further study.

We observed no channel formation in the compost but, as a result of settling, a small part of the process air went up via the sides of the tunnel. The model does not take this into account.

## Acknowledgement

We thank Dr. J. Batista for his assistance in tunnel measurements and Mr. J.G.M. Amsing for providing us with $O_2$ and $CO_2$ data.

## References

Alexander, M. 1977. Introduction to soil microbiology. 2nd ed. Wiley, New York, 467 pp.

Beukema, K.J., S. Bruin, & J. Schenk, 1982. Heat and mass transfer during cooling and storage of agricultural products. *Chemical Engineering Science* 37: 291–298.

Derikx, P.J.L., H.J.M. Op den Camp, C. Van der Drift, L.J.L.D. Van Griensven & G.D. Vogels, 1990a. Odorous sulphur compounds emitted during production of compost used as a substrate in mushroom cultivation. *Applied and Environmental Microbiology* 56: 176–180.

Derikx, P.J.L., H.J.M. Op den Camp, C. Van der Drift, L.J.L.D. Van Griensven & G.D. Vogels, 1990b. Biomass and biological activity during the production of compost used as a substrate in mushroom cultivation. *Applied and Environmental Microbiology* 56: 3029–3034.

Gerrits, J.P.G., 1982. Circulation in tunnels with *A. bitorquis*. (In Dutch). *De Champignoncultuur* 26: 111–115.

Gerrits, J.P.G., 1988a. Nutrition and compost. In: L.J.L.D. Van Griensven (Ed), The cultivation of mushrooms. Darlington Mushroom Laboratories Ltd., Rustington, pp. 29–72.

Gerrits, J.P.G., 1988b. Compost treatment in bulk for mushroom growing. *The Mushroom Journal* 182: 471–475.

Gerrits, J.P.G., H.C. Bels-Koning & F.M. Muller, 1967. Changes in compost constituents during composting, pasteurization and cropping. *Mushroom Science* 6: 225–243.

Gerrits, J.P.G. & L.J.L.D. Van Griensven, 1990. New developments in indoor composting (tunnel process). *The Mushroom Journal* 205: 21–29.

Gray, K.R., K. Sherman & A.J. Biddlestone, 1971. A review of composting – part 1. *Process Biochemistry* 6(6): 32–36.

Hogan, J.A., F.C. Miller & M.S. Finstein, 1989. Physical modelling of the composting ecosystem. *Applied and Environmental Microbiology* 55: 1082–1092.

Krischer, O. & H. Esdorn, 1956. Die Wärmeübertragung in feuchten, porigen Stoffen verschiedener Struktur. *Forschung auf dem Gebiete des Ingenieurswesens* 22(1), Düsseldorf, Germany.

Kuter, G.A., H.A.J. Hoitink & L.A. Rossman, 1985. Effects of aeration and temperature on composting of municipal sludge in a full-scale vessel system. *Journal of Water Pollution Control Federation* 57: 309–315.

Lapidus, L. & G.F. Pinder, 1982. Numerical solution of partial differential equations in science and engineering. Wiley, New York, 677 pp.

Lentz, C.P., L. Van den Berg & S.R. MacCullough, 1971. Study of factors affecting temperature, relative humidity and moisture loss in fresh fruit and vegetable storages. *Journal Institut Canadien de Technologie Alimentaire* 4: 146–153.

Lomax, K.M., N.E. Collins & C.M. Dennemy, 1984. Simulating mushroom compost heat production (compost energy conversion). *Biocycle* 25: 38–40.

Moretti, G. & M. Abbett, 1966. A time-dependent computational method for blunt body flows. *AIAA Journal* 4: 2136–2141.

Ohm, A., 1972. Selfheating and drying proceses in hay. (In Dutch, with English summary). Ph.D. thesis, Technical University Delft, The Netherlands, 183 pp.

Randle, P.E., 1977. Aeration requirement in composting. In: W.A. Hayes (Ed.), Composting, proceedings second seminar mushroom science. Mushroom Growers Association / Maney & Son, Leeds, pp. 25–31.

Randle, P.E. & P.B. Flegg, 1985. The effect of the duration of composting on compost density and the yield of mushrooms. *Scientia Horticulturae* 27: 21–31.

Schisler, L.C., 1982. Biochemical and mycological aspects of mushroom composting. In: P.J. Wuest & G.D. Bengtson (Ed.), Penn State handbook for commercial mushroom growers. Pennsylvania State University, pp. 3–8.

Sinden, J.W. & E. Hauser, 1950. The short method of composting. *Mushroom Science* 1: 52–59.

Speckhart, F.H. & W.L. Green, 1976. A guide to using CSMP: the continuous system modelling programm. Prentice-Hall, New Jersey, 325 pp.

Spohn, E., 1970. Composting by artificial aeration. *Compost Science* 11(3): 22–23.

Straatsma, G., J.P.G. Gerrits, M.P.A.M. Augustijn, H.J.M. Op den Camp, G.D. Vogels & L.J.L.D. Van Griensven, 1989. Population dynamics of *Scytalidium thermophilum* in mushroom compost and stimulatory effects on growth rate and yield of *Agaricus bisporus*. *Journal of General Microbiology* 135: 751–759.

Van Loon, W., 1991. Heat and mass transfer in frozen porous media. Ph.D. thesis, Agricultural University Wageningen, Wageningen, 204 pp.

## Notation

I, Input, and O, output, parameters in the model (input given at the start of calculations only, or are intermittently calculated as output and re-used in calculation cycles).

| Symbol | Description | Unit | I/O |
|---|---|---|---|
| $A$ | Surface area of tunnel walls | $m^2$ | I |
| $c_{p,a}$ | Specific heat of water saturated air | $J\,kg^{-1}\,K^{-1}$ | I |
| $c_{p,c}$ | Specific heat of compost | $J\,kg^{-1}\,K^{-1}$ | I |
| $c_{p,d}$ | Specific heat of organic solids | $J\,kg^{-1}\,K^{-1}$ | I |
| $c_{p,w}$ | Specific heat of water | $J\,kg^{-1}\,K^{-1}$ | I |
| $C_{ox}$ | Concentration of oxygen in air | $kg\,m^{-3}$ | O |
| $C_w$ | Concentration of water vapour in air | $kg\,m^{-3}$ | O |
| $D_{ox}$ | Coefficient of diffusion of oxygen in air | $m^2\,s^{-1}$ | I |
| $D_w$ | Coefficient of diffusion of water vapour in air | $m^2\,s^{-1}$ | I |
| $f$ | Convective heat transfer | $W\,m^{-2}$ | O |
| $h$ | Height of compost | m | I/O |
| $H$ | Heat of evaporation of water | $kJ\,kg^{-1}$ | I |
| $K$ | Thermal conductivity tunnel wall (polyurethane foam) | $W\,m^{-1}\,K^{-1}$ | I |
| $m_t$ | Total mass of compost | kg | I/O |
| $m_d$ | Mass of dry matter | kg | I/O |
| $m_{ox}$ | Mass of oxygen gas | kg | I/O |
| $M$ | Molecular weight of water, $M = 18$ | $kg\,kmol^{-1}$ | I |
| $Pé$ | Péclet number, $Pé = v \cdot \Delta z / D_w$ | – | O |
| $q$ | Conductive heat transfer | $W\,m^{-2}$ | O |
| $R$ | Gas constant, $R = 8310$ | $J\,kmol^{-1}\,K^{-1}$ | I |
| $R_{ox}$ | Consumption rate of oxygen | $kg\,m^{-3}\,s^{-1}$ | O |
| $R_w$ | Evaporation rate of water | $kg\,m^{-3}\,s^{-1}$ | O |
| $t$ | Process time | s or day | I |
| $T$ | Actual compost temperature | °C | I/O |
| $T_0$ | Actual ambient temperature | °C | I |
| $v$ | Superficial velocity of air | $m\,s^{-1}$ | O |
| $V_a$ | Volume of air | $m^3$ | O |
| $V_d$ | Volume occupied by dry matter | $m^3$ | I/O |
| $V_t$ | Total compost volume | $m^3$ | I/O |
| $V_w$ | Volume occupied by water | $m^3$ | I/O |
| $W$ | Heat production of compost (dry matter) | $W\,kg^{-1}$ | I/O |
| $z$ | Height in compost, $z = 0$ is bottom | m | I |
| **Greek Letters** | | | |
| $\alpha$ | Heat transfer coefficient | – | I |
| $\beta$ | Tortuosity of compost | $m\,m^{-1}$ | I |
| $\gamma_a$ | Specific density of the gas phase, based on the | $kg\,m^{-3}$ | I/O |

| | | | |
|---|---|---|---|
| | space occupied by the gas phase only | | |
| $\gamma_d$ | Specific density of dry organic matter, based on the space occupied by dry matter only | $kg\ m^{-3}$ | I |
| $\gamma_w$ | Specific density of water, based on the space occupied by water only | $kg\ m^{-3}$ | I |
| $\delta$ | Thickness of insulation of wall | m | I |
| $\varepsilon$ | Porosity of compost | $m^3\ m^{-3}$ | I/O |
| $\lambda$ | Thermal conductivity of compost | $W\ m^{-1}\ K^{-1}$ | I/O |
| $\rho_c$ | Bulk density of compost, based on the space occupied by all phases | $kg\ m^{-3}$ | I/O |
| $\rho_d$ | Density of organic solids, based on the space occupied by all phases | $kg\ m^{-3}$ | I |
| $\rho_{ox}$ | Density of oxygen, based on the space occupied by all phases | $kg\ m^{-3}$ | I/O |
| $\rho_w$ | Density of water, based on the space occupied by all phases | $kg\ m^{-3}$ | I |
| $\chi$ | Moisture content of compost | $kg\ kg^{-1}$ | I/O |

Subscripts

| | |
|---|---|
| *a* | air |
| *c* | compost |
| *d* | dry matter / organic solids |
| *p* | at constant pressure |
| *ox* | oxygen |
| *w* | water |
| *t* | total |
| *0* | ambient |